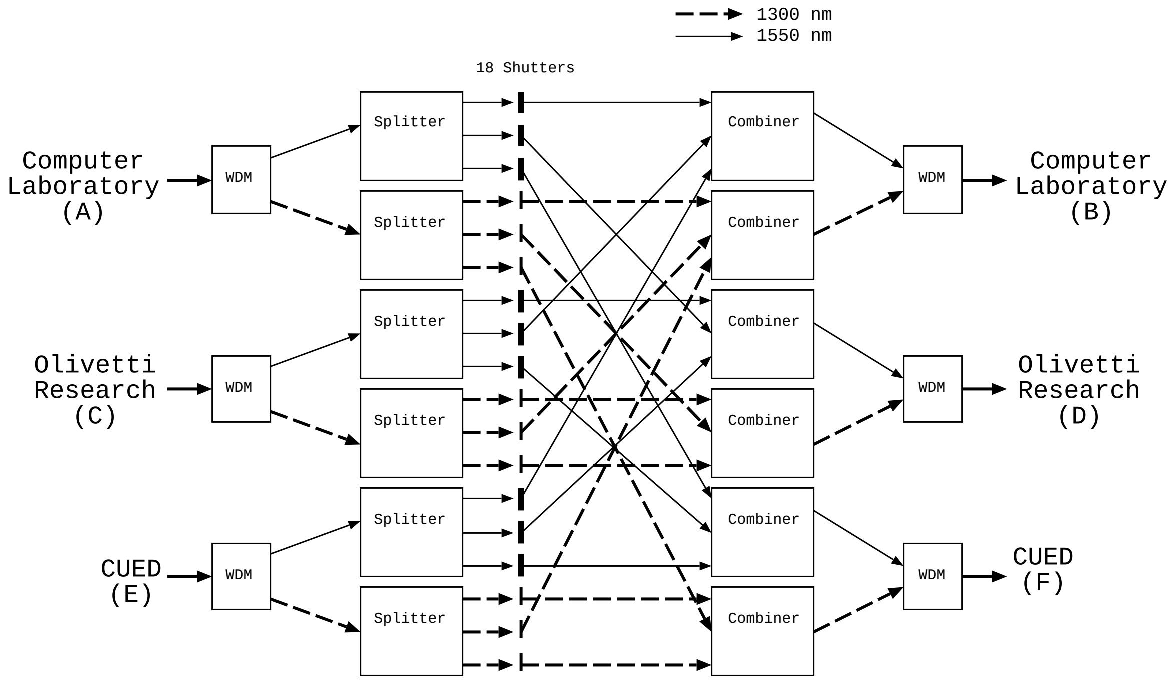

Figure 1: First generation optical space-wavelength crossbar switch.

Optical Switching Testbed Report

1 Introduction

The Optical Switching Testbed was a one and a half year programme of research to establish a simple, free-space multi-wavelength, multi-site, fibre-optic circuit switch testbed in a real ATM network. This will subsequently be used to test more advanced switches and network control protocols.

The system was constructed from a mixture of locally built and bought in components, and operated over the Granta network of fibres between three distinct sites: Olivetti Research Ltd (ORL), the Computer Laboratory (CL) and the Dept of Engineering (CUED). A performance study of the testbed was undertaken as part of the project.

2 Experimental Switch

The optical crossbar switch was constructed with two guiding design criteria:

(i). to provide a simple, robust switch to facilitate network testing,
(ii). to enable progressive introduction of liquid crystal-based (LC) switches and free-space optics to provide a scalable route to more complicated switches.

The first generation switch was based on passive optical fibre splitters, combiners and diplexers, with 18 shutters providing the active switching components. Figure 1 shows the configuration. The shutters form two 3x3 crossbars, one for 1300nm wavelength and a second for 1550nm wavelength. The shutters consist of a 3cm free space optical path with an LC panel in the middle. Each panel is electrically switched between a clear transmissive state and a blocking scattering state. The switch was populated in various test configurations using 6 functional shutters, and is controlled remotely using the `telnet` protocol over the internet. A PC running Linux acted as the switch controller at CUED.

2.1 Data sources and sinks

Figures 2 and 3 show schematics of the digital data sources and data sinks used to transmit data through the switch. They consist of an ARM processor, a field programmable logic array and a serial/parallel converter. These provide flexible control of the line code and error statistics to be collected. The serial

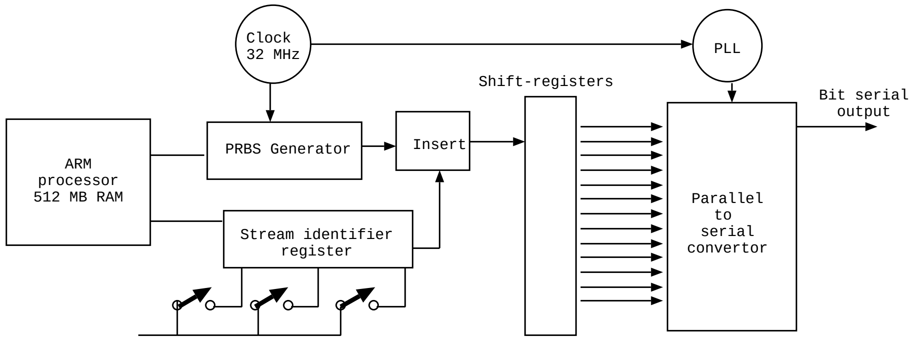

Figure 2: Data source configuration

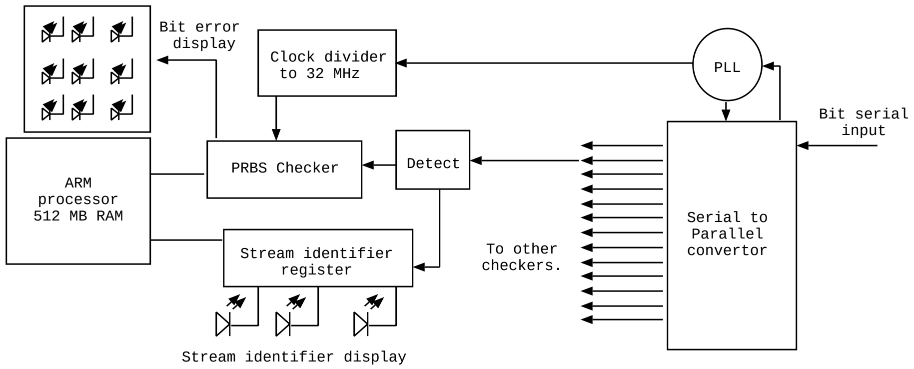

Figure 3: Data sink configuration

rates available are 32, 512 and 1000 Mbps according to choice of transmission card. Six of these systems were built (although only one 1000 Mbps card is complete to date).

The serial electrical signal was converted to either a 1300nm or 1550nm optical signal with a launch power of between 0.5 and 2mW according to the laser transmitter card used. Six laser cards were built. The 1300nm transmitter wavelength can be fine-tuned by control of peltier heat pumps for experiments with high-density WDM, but this feature has not yet been fully tested. The lasers were operated with a modulation depth of 100% at 32 Mbaud, but owing to the non-arrival and late arrival of various laser driver chips, a modulation index of only about 20% was available for the higher rates, thus immediately losing some 6dB of link margin.

The optical to electrical conversion uses wavelength insensitive PIN-diode transimpedance receivers. The receivers have a half-power bandwidth of about 650MHz, meaning that additional noise is present at the 32 Mbaud rate and some ISI is present for the 1Gbps rate. The effects of correct filtering for the 32 Mbaud rate were briefly investigated, and found to make about 1.5dB difference in noise margin, as expected. The link noise level is dominated by the receiver self-noise, which is 3.5pA per $\sqrt{\mathrm{Hz}}$, and the sensitivity of the overall receiver is -37.5dBm for an error rate of 1 in $10^{7.5}$. With a 1mW laser and 100% modulation, this was also the nominal loss budget for the optical plant.

The data pattern actually used consists of a $2^{15} - 1$ pseudo-random bit sequence with a presettable 3-bit stream identifier inserted following a particular point. The combined pattern was NRZI encoded to avoid polarity problems. The stream identifier was set differently at each source and so could show correct operation of the optical switching function. For serial rates above 32 Mbaud, the serial stream consisted of interleaved repeat copies of the data pattern, although spaced with many bits delay so that adjacent bits were not correlated. The error rates were measured using a binary LED display of errors (both one-to-zero and zero-to-one errors were logged). The LED display had 16 bits which allowed error rates between about 0.01Hz and 1kHz to be accurately determined by eye.

2.2 Passive optical fibre plant

The testbed switch contains six WDM 1300/1550nm fibre (de)multiplexers and twelve passive 1:3/3:1 fibre splitters/combiners. The additional Granta network passive plant includes WDM fibre components at each source and sink, and separate transmit (Tx) and receive (Rx) monomode fibres from CL and ORL to the switch at CUED. The 4 Granta fibres introduce multiple splice losses as shown in table 1 (see attached appendix). The CUED Tx and Rx fibres were implemented as short optical patch cables. Loss measurements of the plant losses are subject to a certain amount of variability owing to some of the monomode fibre connectors mating variability. However, here we report the best results, where a connector had to be occasionally tightened or refitted.

The Granta fibre losses were measured at both wavelengths using an optical power meter. Measurement of the loopback loss from the CL Tx to CL Rx fibres transmitting a 0dBm 1300nm source through all switch components except the LC panel, compared with the loss figure when the switch was bypassed with a patch lead, indicated that the loss in the switch passive components is 16.7dB. The received power with all other switch paths disconnected, was −23.7dBm.

The total round-trip delay from the CL source to sink was measured as 13.5μs, indicating a total fibre length of 2.4km. The predicted loss of this length of fibre would be less than 1dB, and hence there is significant loss from splices in the Granta plant and from the termination connectors. Note: The total link power budget for the working system also includes the intrinsic and excess losses for the WDM splitters and combiners at each source and sink, together with the insertion loss of the LC panel in its transparent state. Table 2 shows the performance of one of the WDM diplexers used to combine or demultiplex the 1300nm and 1550nm wavelength channels at the sources and sinks. The excess loss of approximately 1dB includes an additional fibre FC-PC connector.

2.3 LC shutter performance

Experimental and theoretical consideration was given to LC electro-optic effects that can operate with high efficiency at 1300nm and 1550nm wavelengths with polarisation insensitivity. Measurements were made on a wide range of effects in nematics, cholesterics, smectics and polymer-dispersed liquid crystal devices. A number of these effects could be optimised for efficient operation, several exhibiting electro-optic bistability. The system selected for the crossbar shutter was the light scattering effect produced by the planar to homeotropic transition in a cholesteric liquid crystal of pitch around 1μm (the materials used were Merck E7 doped with CB15). The switching characteristics of the LC shutters vary significantly with driving scheme. At 1300nm, a high contrast ratio of 23dB can be produced within a latency of 50ms, but a compromise was required to maximise performance at 1550nm wavelength. The new drive scheme resulted in a slower switching characteristic (fig. 4), but high isolation at both wavelengths (table 3). The insertion losses of 7.4 and 5.8dB are acceptable and the extinction ratio of 27.9dB (the worse of the two wavelengths) is more than sufficient to eliminate bit errors from crosstalk for amplitude modulated data.

3 Switch Performance

A total of 6 LC shutters were available to fill the 18 possible places in the prototype switch. These were installed in three test configurations:

(i). a 3 source by 2 sink optical crossbar switch at 1300nm,
(ii). a 3 source by 2 sink optical crossbar switch at 1550nm,
(iii). a 2 source by 1 sink dual wavelength switch.

Two sets of measurements were made with configuration (i) to determine the switch insertion losses and crosstalk isolation. Table 4 shows the received optical powers with each source active in turn. Asterisks in the table represent 'open' paths through the switch. Clearly the results have satisfactory loss and crosstalk margins, meeting the design specification of -13dB isolation. All 3 sources were activated during the second measurement (table 5), and no bit errors were recorded after the desired pattern of connectivity had been achieved by remotely programming the shutters across the internet. A full 3x3 crossbar was not possible because of the availability of only 6 shutters.

Table 6 shows that the performance of the system as a 1550nm crossbar switch also has satisfactory margins. The CUED 1550nm could not be modulated and thus no measurement could be made with all

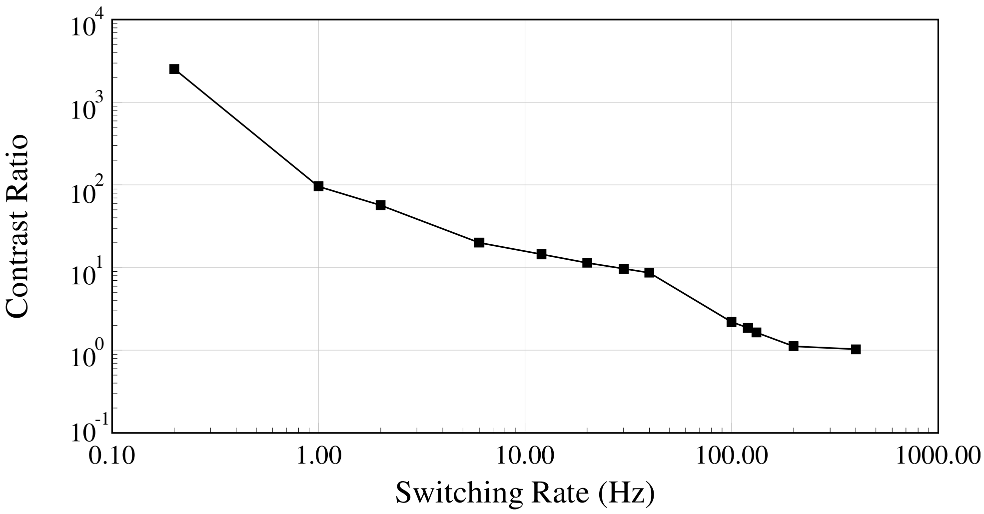

Figure 4: Switching frequency response of LC shutter.

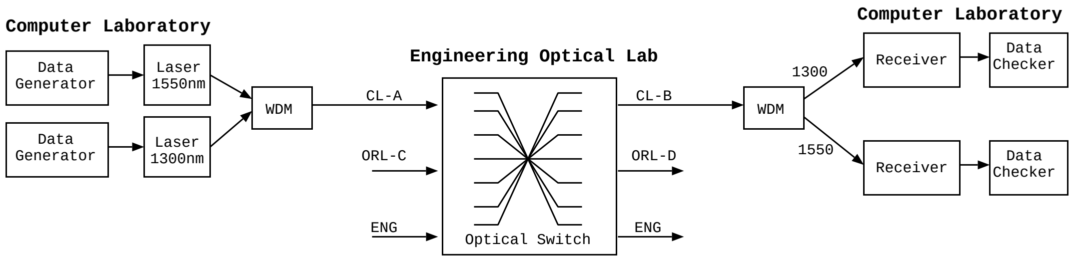

Figure 5: WDM configuration (iii).

3 sources active.

Data streams at both 1300nm and 1550nm were routed simultaneously through the switch with configuration (iii), using 4 LC shutters. Table 7 shows the network performance. Note that the two sources did not have the same power, so comparisons of absolute loss between wavelengths are not possible. However, the passive WDM fibre splitters in the switch provide excellent wavelength isolation, and the switch clearly has usable transmission loss and extinction. Four WDM experiments were conducted to characterise the dual wavelength performance:

(i). two wavelength channels feeding the network from the same site,
(ii). two wavelength channels from distinct sites combined in the switch,
(iii). as (i), but wavelength channels split again at the receiver, ie. loopback (fig. 5),
(iv). as (ii), but wavelength channels split again at the receiver (fig. 6).

All four WDM configurations were demonstrated at 32 Mbaud, and the switch control of the streams was perfect–perfect in the sense that all shutters had the desired effect and no side effects occurred. Therefore the full 3x3 dual wavelength switch was effectively proven, since the losses in the 3x3 system are fully represented, and calculation shows the crosstalk penalty of 3 sources instead of 2 is completely insignificant.

4 Further Experiments to Examine Scalability Issues

4.1 Space switching experiments

The major achievement of this study was the discovery that chiral smectic C^* (ferroelectric) liquid crystals, when operated as phase pixels in the Fourier plane of a lens, could be used to construct a polarisation insensitive beam-steering switch independent of the optical thickness of the cell and of the molecular FLC switching angle [1]. Thus in future switching architectures, the passive fan-out and fan-in

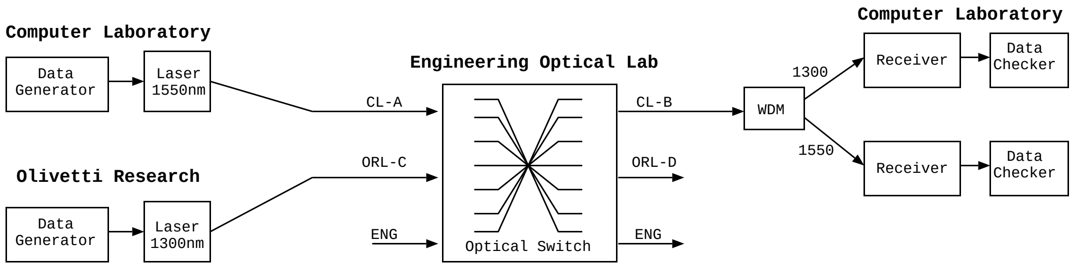

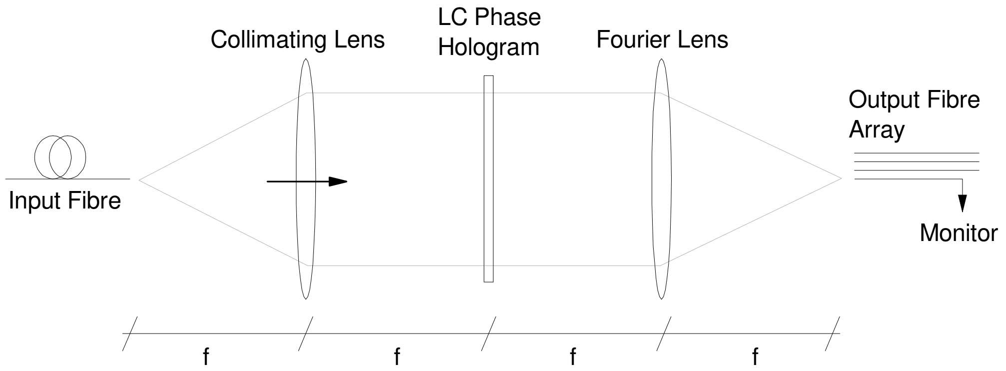

Figure 7: Holographic switch configuration.

performed by the fibre splitters in the testbed switch can be replaced by active $1:N$ and $N:1$ routeing switches in a dilated crossbar (router-selector) architecture. The approach promises enhanced scalability for large fibre switching matrices, and will be pursued under a new DTI/EPSRC LINK programme [2]. As a demonstration for this project, $1:3$ and $3:1$ switches were tested for the 1550nm wavelength half of the crossbar. Results are shown in figure 8.

4.2 WDM experiments

A number of experiments were performed to facilitate future expansion of the switch to greater numbers of WDM channels. In the light of advances in telecommunications technology, it was decided to use an Erbium doped fibre amplifier (EDFA) rather than a semiconductor amplifier. The EDFA has a gain window of about 40 nm centred around 1540nm wavelength. During the course of the project, the ITU has specified 16 WDM channels spaced by 0.8nm (100GHz) in this band. The advances at CUED in the design of reconfigurable gratings/holograms in FLC materials has led to the demonstration of a digitally programmable tuneable filter with a wavelength stability of 0.1nm [3]. A typical result is shown in fig. 9. The intention is to develop the filter in a future project so that it can be used to replace current fixed diffraction grating demultiplexers. A further experiment has used the filter in conjunction with the EDFA to create a digitally tuneable laser. This work was partially supported by OST, but also by a further EPSRC project, POETS. The result is a wavelength agile laser which can be tuned to more than 20 WDM channels in the EDFA gain window. Successive tuned lasing modes are shown in fig. 10. The laser promises to considerably expand the functionality demonstrated on OST, but would require an external modulator and drive circuitry to be integrated into the testbed. It is hoped that this would be achieved under a second phase proposal.

5 Partner Contributions

The Engineering Department provided space and manpower for aspects of the work, especially the construction and testing of the optics and other testbed switch components. The Computer Laboratory provided space and manpower for aspects of the work, especially the construction and testing of the sources and sinks, and the network testing. Olivetti Research contributed a number of mono-mode

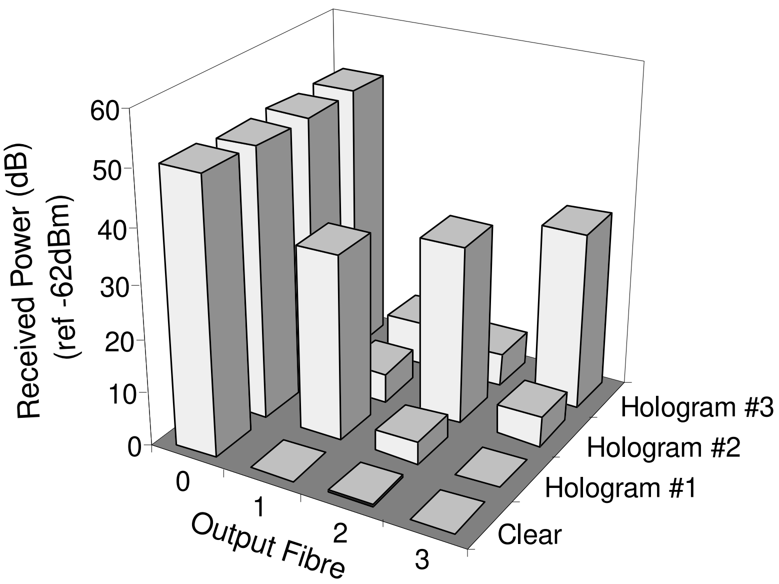

Figure 8: Beam steering received powers.

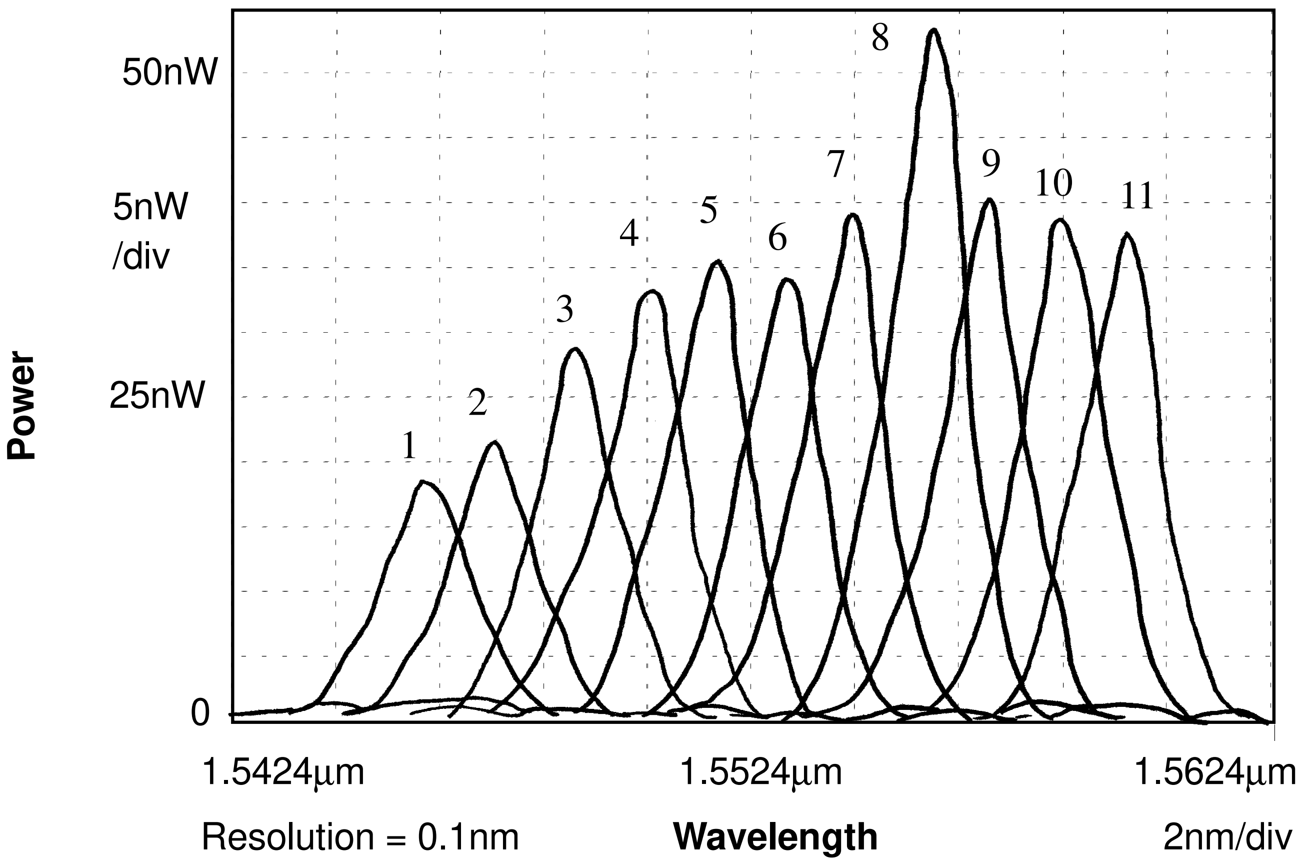

Figure 9: Spectral transmissions of holographically tuned wavelength filter.

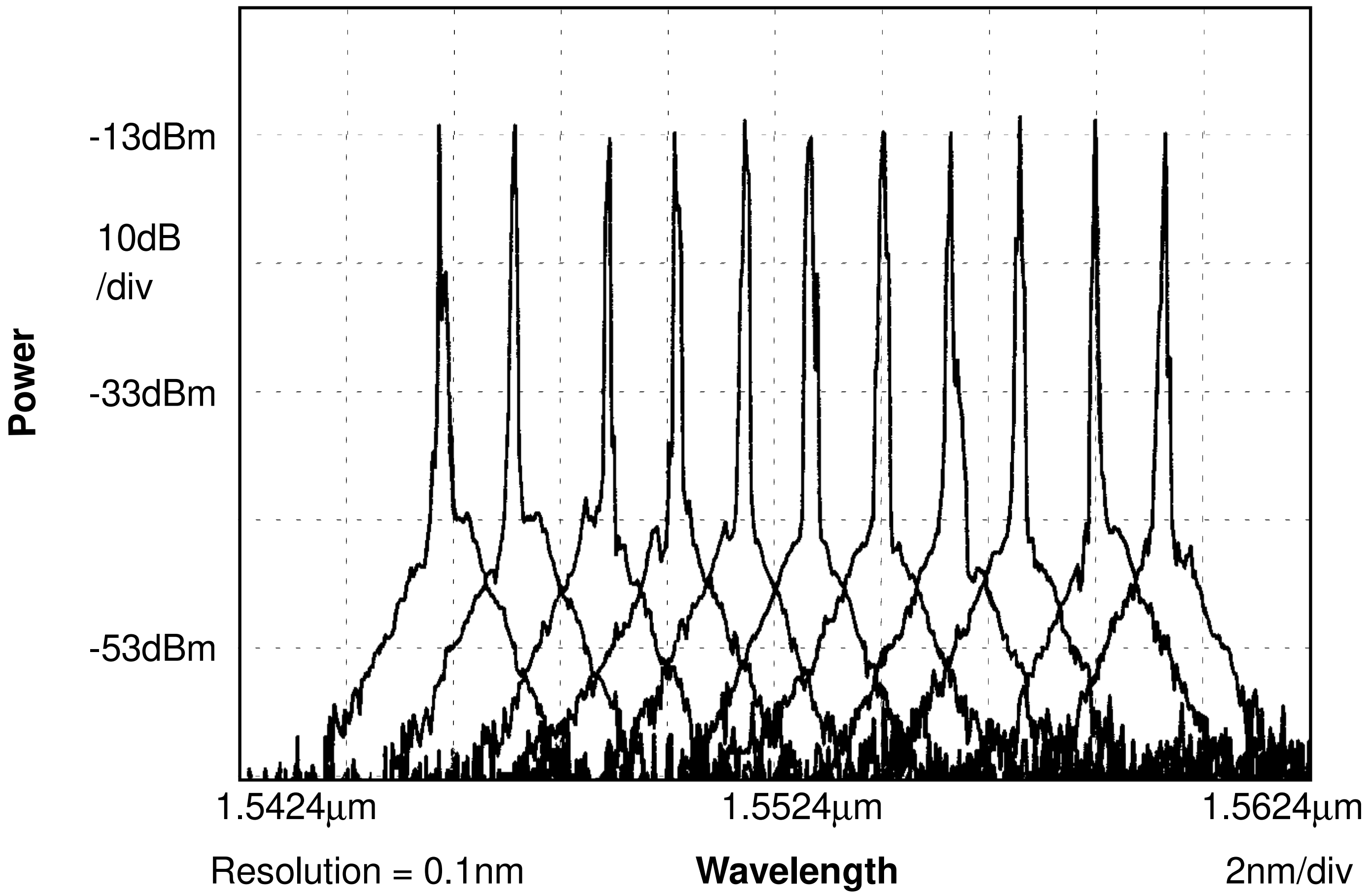

Figure 10: Successively tuned lasing wavelengths (1.3nm steps).

optical components and access to test gear, including a 10GHz sampling scope, fusion splicer and power meter. ORL also funded the development of the additional laser sources at the Computer Laboratory. This work was funded by EPSRC and ORL.

6 Summary

The components for an effective optical switching testbed were put together, including sources, sinks, control computer and metropolitan fibre plant. A 3x3 space and dual wavelength crossbar has been constructed and tested in a campus network.

A new polarisation-insensitive beam-steering $1:N$ ferroelectric liquid crystal switch has been developed and demonstrated. With an appropriate interface, sub-millisecond ($100\mu s$) latency should be possible. WDM experiments have demonstrated a tuneable filter/laser technology capable of supporting in excess of the 16 ITU recommended channels in the EDFA window at $1.54\mu m$. We can now proceed to use the optical testbed facility to test these, and more sophisticated switches and network control protocols.

References

[1] S.T. Warr and R.J. Mears. Polarisation insensitive operation of ferroelectric liquid crystal devices. *Electronics Letters*, 31(9):714–716, 1995.

[2] DTI/EPSRC LINK Photonics. Reconfigurable optical switches for aerospace and telecommunications systems (ROSES). Ref. GR/K84226.

[3] M.C. Parker, S.T. Warr, and R.J. Mears. Tunable holographic wavelength filter. In *OSA Topical Meeting on Spatial Light Modulators and Applications*, Salt Lake City, Utah, March 12, 1995.

Acknowledgements

Thanks to Dr T.B. Davey, Dr T.D. Wilkinson and I.D. Springle for their practical advice and for making the LC cells used in the testbed switch.

Appendix A: Switch Characterisation

A.1 Passive fibre plant losses

Fibre	Loss at 1300nm (dB)	Loss at 1550nm (dB)
CL Tx	-3.4	-3.0
CL Rx	-6.7	-3.7
ORL Tx	-7.8	-8.3
ORL Rx	-4.2	-3.9

Table 1: Granta network fibre losses.

Source connected to:	Insertion loss (dB) (1300nm source)	Insertion loss (dB) (1550nm source)
1300nm Input	4.1*	31.0
1550nm Input	32.0	3.9*

Table 2: Performance of one of the source/sink WDM diplexers with connectors.

A.2 LC shutter performance

Wavelength	Configuration	Relative Rx Power (dB)
1300nm	no shutter	0.0
	open	-7.4
	blocking	-35.3
1550nm	no shutter	0.0
	open	-5.8
	blocking	-34.5

Table 3: Typical insertion loss measurements for an LC shutter optimised for both wavelengths.

A.3 3 source by 2 sink optical crossbar switch at 1300nm

Tx Source	Tx Path	CL Rx Power (dBm)	ORL Rx Power (dBm)
CL	none	-59.9	-55.0
(+0.4dBm)	CL-CL	-19.3*	-55.0
	CL-ORL	-58.1	-25.2*
ORL	none	-58.0	-58.9
(+0.7dBm)	ORL-CL	-31.6*	-58.9
	ORL-ORL	-57.6	-29.6*
CUED	none	-50.6	-52.3
(+0.7dBm)	CUED-CL	-21.1*	-52.3
	CUED-ORL	-49.8	-20.7*

Table 4: Received optical powers – Each source activated in turn.

Tx Path	CL Rx Power (dBm)	ORL Rx Power (dBm)
none	-50.2	-49.7
CL-CL	-19.1*	-49.7
CL-ORL	-50.2	-25.0*
ORL-CL	-31.2*	-50.2
ORL-ORL	-50.2	-29.2*
CUED-CL	-21.1*	-50.4
CUED-ORL	-50.1	-20.7*
CL-CL + ORL-ORL	-19.1*	-29.2*
CL-CL + CUED-ORL	-19.0*	-20.7*
ORL-CL + CL-ORL	-31.2*	-25.0*
CUED-CL + CL-ORL	-21.1*	-25.1*
CUED-CL + ORL-ORL	-21.1*	-29.2*
ORL-CL + CUED-ORL	-31.2*	-20.7*

Table 5: Received optical powers – All three sources active.

A.4 3 source by 2 sink optical crossbar switch at 1550nm

Tx Source	Tx Path	CL Rx Power (dBm)	ORL Rx Power (dBm)
CL	none	-56.7	-62.0
(-4.4dBm)	CL-CL	-28.3*	-62.1
	CL-ORL	-56.8	-28.3*
ORL	none	-57.3	-61.4
(-4.4dBm)	ORL-CL	-32.3*	-61.4
	ORL-ORL	-57.3	-32.2*
CUED	none	-48.5	-52.5
(0.4dBm)	CUED-CL	-23.3*	-52.5
	CUED-ORL	-48.5	-27.4*

Table 6: Received optical powers – Each source activated in turn.

A.5 2 source by 1 sink dual wavelength switch

Tx Path	Tx Wavelength	1300nm Shutter (dBm) (open/blocked)	1550nm Shutter (dBm) (open/blocked)
CL-CL	1300nm	-25.6* / -61.0	-61.5 / -63.3
	1550nm	-61.0 / -61.0	-31.6* / -63.3
ORL-CL	1300nm	-25.5* / -50.4	-64.9 / -69.0
	1550nm	-50.4 / -40.4	-35.0* / -69.0

Table 7: Received optical powers – Performance of the 4 shutters used in the dual wavelength tests.